Journal of the Serbian Chemical Society
JSCS-info@shd.org.rs • www.shd.org.rs/JSCS

ACCEPTED MANUSCRIPT

Journal of the Serbian Chemical Society
JSCS-info@shd.org.rs • www.shd.org.rs/JSCS
J. Serb. Chem. Soc. **00(0)** 1-18 (2026)
JSCS–13823
Original scientific paper
Published DD MM, 2026

Voltammetric study of a detergent-stable *Actinomadura keratinilytica* lipase CPT29-cross-linked GA/BSA platinum biosensor

SELMA BOUNOUR[1], FATIHA BENAMIA[1]*, NOURA SEMACHE[1], SAIDA ZOUGAR[2], RAHMA BENYAHIA[2], NOUREDDINE DADDA[3], AND ALI LADJAMA[4]

[1]*Laboratory of Applied Organic Chemistry, Chemistry Department, Faculty of Sciences, Badji Mokhtar University, P.O. Box 12, 23000 Annaba, Algeria,* [2]*Laboratory of Environmental Engineering, Process Engineering Department, Faculty of Technology, Badji Mokhtar University, P.O. Box 12, 23000, Annaba, Algeria,* [3]*Laboratory of Synthesis and Organic Biocatalysis, Chemistry Department, Faculty of Sciences, Badji Mokhtar University, P.O. Box 12, 23000 Annaba, Algeria, and* [4]*Laboratory of Applied Biochemistry and Microbiology, Biochemistry Department, Faculty of Sciences, Badji Mokhtar University, P.O. Box 12, 23000, Annaba, Algeria.*

(Received 7 March; revised 17 April; accepted 23 July 2026)

Abstract: This study describes the immobilization of a native lipase (LCPT29) from *Actinomadura keratinilytica* strain CPT29 isolated from poultry compost in north-east of Algeria in order to detect ester pollutants in an aqueous environment. For this purpose this detergent-stable lipase was immobilized with glutaraldehyde as a cross-linker, in the presence of bovine serum albumin (BSA) onto a platinum (Pt) electrode. The prepared enzyme membrane was characterized by FT-IR spectroscopy, confirming its formation network, and its coating the Pt-electrode by evaluating electrochemical changes using cyclic voltammetry. The effectiveness of the cross-linked enzyme membrane-coated working electrode was evaluated electrochemically by detecting propyl 4-hydroxybenzoate (PHB) as a model analyte. Under optimal conditions and at an applied potential of -250 mV, the LCPT29-based biosensor showed a linear response over the concentration range from10^{-14} to 10^{-8} mol L^{-1} (r = 0.991), with a detection limit of 10^{-14} mol L^{-1}. The biosensor exhibited high sensitivity (0.0327 mA L mol^{-1}), good stability (RSD = 0.37 %) and significant selectivity as well as the ability to analyze trace amounts of PHB in real water samples, demonstrating its potential for electrochemical biosensing applications.

Keywords: immobilization; enzyme membrane; biosensor; electrochemical; ester pollutant.

* Corresponding author. E-mail: fatiha.benamia@univ-annaba.dz
https://doi.org/10.2298/JSC260307038B

INTRODUCTION

Due to their catalytic nature, which accelerates biochemical reactions in living organisms, enzymes play a crucial role in many biotechnological applications. They are essential for analytical devices used in various environmental and medical applications, including biosensors and biocatalysis.[1,2] As recognition elements in biodetection, they provide developed biosensors with high detection capabilities, essential characteristics for analyzing target compounds in complex matrices.[3,4] Alongside these technological advances, the application of enzymes in biosensors is a current research area that is increasingly being explored.

Biosensors are devices that combine a biological recognition element, such as an enzyme, with a physicochemical transducer, thus enabling the conversion of a specific biochemical reaction into a measurable signal.[5] Although the exploitation of commercial enzymes is widespread, their use often remains limited by their high cost, availability, and sometimes their stability under specific environmental conditions.[6] As an alternative to commercially produced enzymes, those derived from autochthon microorganisms are cited. A wide variety of microorganisms produce enzymes, which differ in their microbial origin, chemical properties, and mechanisms of action. Generally, microbial enzymes catalyze hydrolysis, oxidation, or reduction reactions.[7] Microbial lipases are the most widely used enzymes in the industrial world because they are more economical, stable and easy to culture.[8]

Lipases (EC 3.1.1.3 triacylglycerol acylhydrolase) are enzymes from the hydrolase group, mainly involved in the degradation of fats.[9,10] They are common in nature and are made by fungi, bacteria, and actinomycetes, as well as plants, animals, and other microorganisms.[11] On an industrial scale, lipases are produced by microbes.[12] Lipase is widely employed for detecting ester-based pollutants due to its catalytic hydrolysis activity.[13] In recent years, many enzyme electrochemical biosensors were conceived, developed, and commercialized as user-friendly and time-saving analytical methods.[14] Their immobilization enhances stability, reusability, and applicability in biosensing systems.[1] Recently, numerous immobilization approaches, such as adsorption, entrapment, covalent binding, and cross-linking, have been examined in the literature.[15]

Exploiting a detergent-stable extracellular lipase from an authochton strain of *Actiomaudura keratinilytica* (CPT29), we developed a platinum-electrode-based enzymatic membrane. This membrane was designed to create a cost-effective, highly sensitive, and selective biosensor for detecting ester-type pollutants in aquatic environments. The lipase was immobilized on a platinum electrode to form an enzymatic membrane, which was characterized by FT-IR spectroscopy and cyclic voltammetry.

EXPERIMENTAL

Chemicals and reagents

BSA (bovine serum albumin 99 %), aqueous solutions of glutaraldehyde (25 % ; w / v), buffer solutions, glycerol (99 %), and ester substrate were purchased from Sigma-Aldrich Chemie GmbH (Munich, Germany).

Enzyme source

In this study, the lipase[16] used as a biological recognition element, was previously produced from *Actinomadura keratinilytica* strain CPT29 [GenBank accession no. KC447297] isolated from poultry compost collected from a local farm in north-east region of Annaba in Algeria.[17]

Apparatus and measurements

Electrochemical analyses were performed using a modular SP-300 potentiostat/ galvanostat (Biologic Science Instruments, France), controlled by EC-Lab software (v11.46) for data acquisition and processing. Measurements were carried out in a three-electrode cell consisting of a platinum working electrode (0.5 cm^2), a platinum wire auxiliary electrode (0.1 cm diameter), and a saturated calomel (SCC) reference electrode. The working electrode had been previously cleaned according to a previously described procedure.[13]

Immobilization procedure

Immobilizing the enzyme on the electrode is a crucial step in biosensor development, as its efficiency depends directly on the fixation method used. Several techniques, such as adsorption, covalent bonding, or encapsulation[18-21], can be employed after prior activation of the surface functional groups. [22,23]

In this study the LCPT29 was immobilized on the surface of platinum electrode by covalent crosslinking in saturated GA vapor with BSA in which the amino groups of a protein are expected to form a Schiff base.[24] During the immobilization, GA acts as a bifunctional cross-linking agent, enabling covalent bonding between the enzyme and the substrate, while BSA is often used as a stabilizing and spacing agent, promoting membrane formation on conductive surfaces. According to a previous study [25], the developed biosensor was prepared by depositing a drop of lipase-based solution containing enzyme / BSA (5 % , w / v) and glycerol (10 %) in 10 mol L^{-1} PBS (90 % and pH 7.4) onto the surface of the Pt-electrode. The modified working electrode was then exposed to the vapor of the saturated GA for 30 minutes, followed by drying at room temperature for another 30 minutes. Finally, it was stored at 4 °C until further use. Scanning electron microscope (SEM, Quanta 250, FEI Company, Eindhoven, Netherlands) and FT-IR transmittance spectra (SHIMADZU IRSpirit-X FTIR) were recorded to confirm the cross-linking and the membrane formation.

Enzyme activity assay

The activity of LCPT29 towards hydrolysis of PHB was measured titrimetrically. The experiment was conducted using a method similar to that described elsewhere with slight modifications.[13] Lipase (50 mg) was added to the PHB (16.7 mol L^{-1}) in 40 mL of PBS (10 mol L^{-1}; pH 8). The mixture was stirred in a water bath at 40°C. The kinetics of the hydrolysis reaction, were monitored using an automatic pH-stat titrator (TitroLine®7000, TitriSoft 3.0, SI Analytics GmbH, Germany). The quantity of the *p*-hydroxybenzoic acid (PHBA) released was titrated adding 0.1 mol L^{-1} of sodium hydroxide to the reaction medium. One unit (1 IU) of hydrolytic activity corresponds to 1 µmol of released acid per minute under the assay conditions used. All determinations were performed in triplicate.

RESULTS AND DISCUSSION

*Characterization of GA/BSA/*LCPT29

FT-IR-spectroscopy analysis

Fig. 1 shows the results of the FT-IR analysis obtained after lipase immobilization. The GA spectrum shows a peak around 1680 cm^{-1} (C=O stretching vibration) attributed to the carbonyl group of the aldehydic function.[26] In the lipase-based membrane spectrum, this peak exhibits a slight shift, suggesting the involvement of glutaraldehyde-derived aldehydes in a chemical reaction. Furthermore, the peaks recorded around 1650 cm^{-1} and 1540 cm^{-1} can be attributed to amide I (C=O stretching vibration) and amide II (C–N stretching and N–H bending), respectively, which are characteristic of proteins.[27] Although a minor contribution of residual GA in the 1650 cm^{-1} region cannot be completely excluded, this band is predominantly associated with the protein components of the membrane (BSA and immobilized enzyme). Indeed, the same band is already observed in the spectrum of pure BSA, confirming its protein origin. Furthermore, the characteristic aldehyde band of free GA around 1680 cm^{-1} is absent or strongly attenuated in the membrane spectrum, suggesting that most of the GA was consumed during the crosslinking reaction with the amino groups of BSA and the enzyme.

The increased intensity of the amide I band in the membrane, compared with that of BSA alone, may be attributed to the combined contribution of BSA and the immobilized enzyme, as well as to structural and chemical modifications induced by GA-mediated crosslinking. These interactions likely involve Schiff base formation and/or imine bond generation between aldehyde groups of GA and amino groups of proteins.[28] Since the amide I region is highly sensitive to the secondary structure of proteins, changes in its intensity and profile may reflect modifications in the local structural environment of the immobilized proteins.[29] The FT-IR spectrum (Fig.1) shows also, a broad absorption between 3000 and 3400 cm^{-1} indicates O–H and N–H bonds stretching vibrations[30], reflecting the presence of hydrophilic groups and bound water. These spectral characteristics together confirm the successful chemical integration of BSA and lipase within the GA-crosslinked membrane[28]. In this region, a weaker band is observed around 2900–3000 cm^{-1}, which may be associated with C–H bond stretching vibrations. On the other hand, the absence of a clearly resolved imine (C=N) band on the spectrum could be attributed to overlap with the intense region of amide I and the low intrinsic intensity of this feature in complex protein matrices.

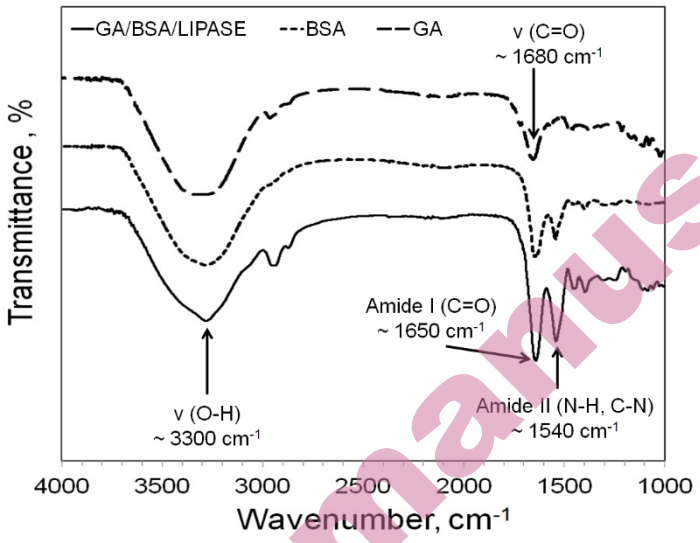

Fig.1. FT-IR spectra of GA, BSA, and the prepared biomembrane GA/BSA/LCPT29

Morphological analysis

In accordance with the method described above, a morphological study was performed to validate the fabrication of the enzymatic membrane on the platinum electrode using SEM analysis under an accelerating voltage of 20 kV, using CBS images at magnifications of 80× and 600× to compare the surface morphology before and after immersion in PHB (Fig. 2a–d). In addition, ETD images at 300× were recorded to further examine the surface changes before and after immersion (Fig. 2a′–b′).

SEM analysis (Fig. 2a–b) revealed homogeneous and stable adhesion of the biomembrane to the platinum electrode surface after deposition. The morphology of the biosensor after immersion in the target analyte was examined (Fig. 2c–d) to assess analyte diffusion to the active sites. The images show a porous structure and cavities within the BSA–GA–enzyme matrix, facilitating analyte penetration and improving access to the active sites, thus promoting mass transfer. These SEM images (Fig. 2c–d) also show brighter areas localized around the membrane pores, suggesting adsorption and/or accumulation of products resulting from the enzymatic hydrolysis of the analyte. Furthermore, ETD images (Fig. 2a′–b′) confirm the surface modification before and after immersion. These observations are consistent with data from the literature[13] and highlight the essential role of porosity in the diffusion of the analyte.

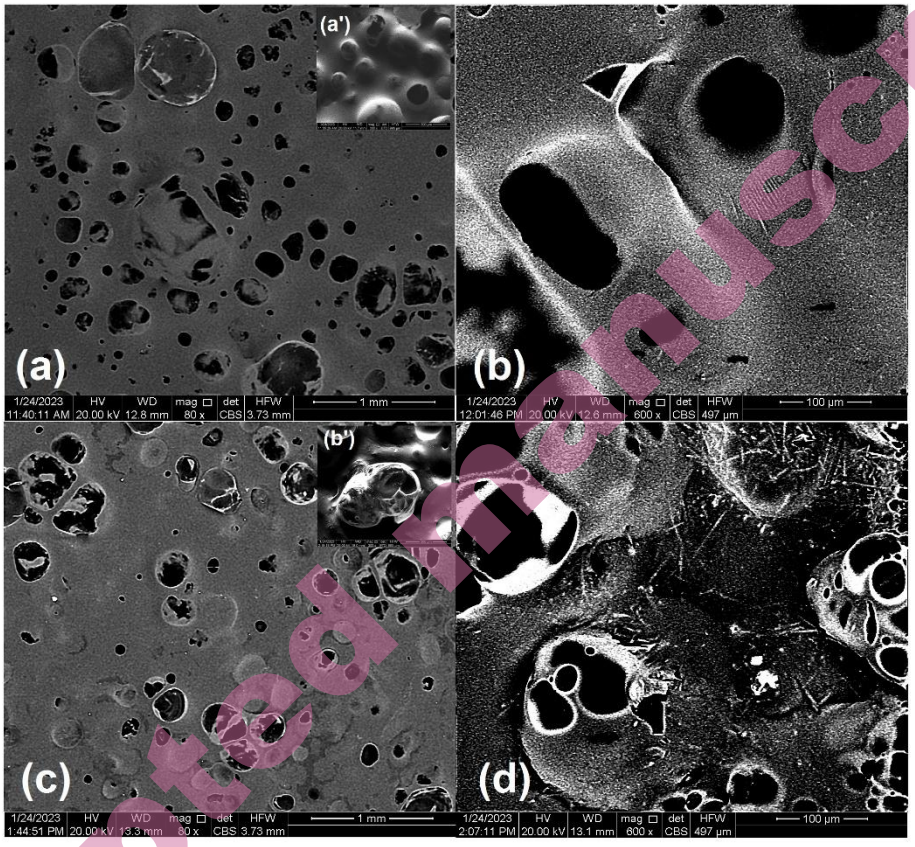

Fig.2. SEM analysis of the platinum electrode coated with a LCPT29-based biomembrane: a and b –before; c and d – after immersion in PHB using CBS images at 80× and 600×. Insets: ETD images at 300× before and after immersion (a′ and b′, respectively).

Cyclic voltammetry analysis

The SEM analysis was then validated by electrochemical characterization of the biomembrane after its deposition on the working electrode. For this purpose the cyclic voltammetry (CV), as a widely used technique in biosensing[31,32], was employed to characterize the surface of a platinum electrode[33] before and after biomembrane deposition. Measurements were performed in a 5 mmol L^{-1} $[Fe(CN)_6]^{3-/4-}$ solution prepared in 10 mol L^{-1} PBS buffer (pH 7.4), with a scanning potential from −0.7 to +0.7 V at 25 mV s^{-1}.

The voltammograms illustrated in Fig. 3a−b show two well-defined anodic and cathodic peaks, indicating a quasi-reversible reversible redox process. The bare electrode (Fig. 3a) exhibits the highest peak currents, indicating rapid electron transfer, while their decrease (Fig. 3b) after modification confirms the formation

of a bioactive layer that limits access to the redox probe, without however, completely blocking electron transfer. [34,35]

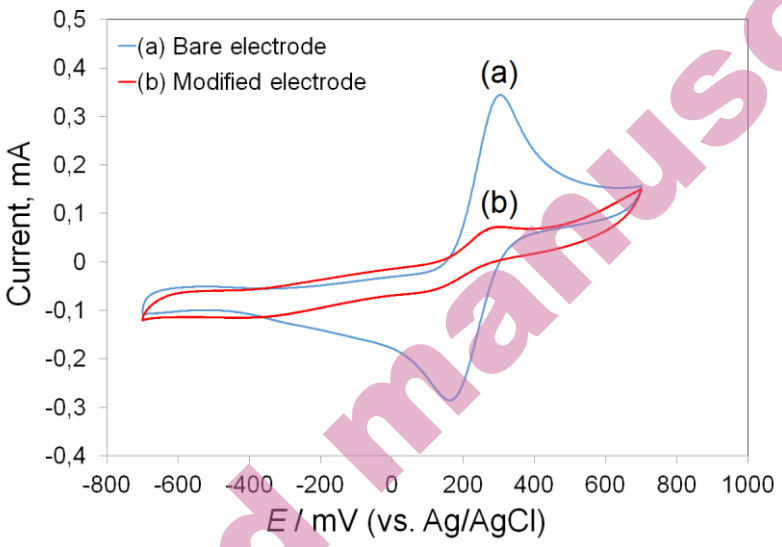

Fig. 3. Cyclic voltamograms recorded for bare and modified electrodes (a and b, respectively), using 5 mmol L^{-1} $[Fe(CN)_6]^{3-/4-}$ in 10 mol L^{-1} PBS buffer (pH 7.4) at a scan rate of 25 mV s^{-1}.

Evaluation of enzymatic activity

In this study, enzymatic hydrolysis of PHB was performed to evaluate the hydrolytic activity of the LCPT29 against this model analyte, prior to its use as a bioreceptor in the development of a novel biosensor. Initially, PHB was converted to PHBA by enzymatic hydrolysis using the titrimetric method described in the experimental section. The proposed reaction mechanism is illustrated in Fig. 4.

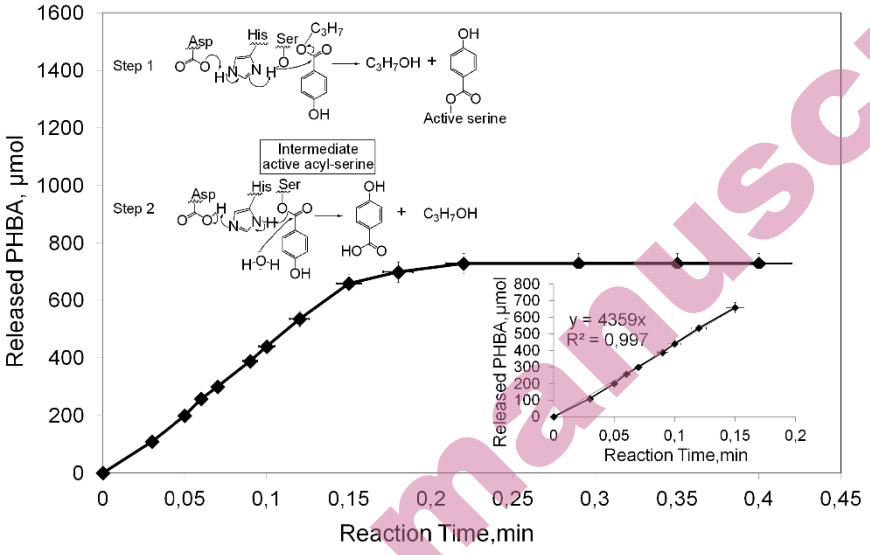

Fig. 4. Kinetic curve recorded for the hydrolysis of PHB to PHBA, catalyzed by LCPT29. The proposed mechanism for the hydrolysis of PHB and the linear portion of the curve are shown in the inset. The reactions were carried out at pH 8 and 40 °C, and their kinetics were continuously monitored using a pH meter. The error bars represent the standard deviation of three measurements.

The hydrolytic activity of the produced LCPT29 was determined from the slope of the linear portion of the kinetic curve, plotted against reaction time (inset of Fig. 4). The enzyme exhibited high activity against the hydrolysis of PHB (4359 IU) and a higher specific activity than previously described enzymes (Table I), highlighting its potential as a novel bioreceptor of a sensitive PHB biosensor.

TABLE I. Comparison of the specific activity of LCPT29 with that of certain enzymes described in the literature, during the hydrolysis of PHB.

Biocatalyst	Specific activity, IU mg^{-1} of enzyme	Reference
LCPT29	90.02 ± 0.05	This work
LPP [a]	53.25 ± 0.02	[10]
PrbA[b]	1.91± 0.03	[32]
rAoPrbA[c]	0.280 ± 0.029	[33]

[a] Lipase from *Porcine Pancreas*; [b] Esterase from *Enterobacter cloacae* strain EM; [c] *Aspergillus oryzae* Esterase.

Optimization of biosensor response

Scan rate effect

To investigate the scan rate dependence and diffusion-controlled kinetics of the modified electrode, the $[Fe(CN)_6]^{3-/4-}$ redox couple was used as a standard quasi-reversible electrochemical probe. Cyclic voltammetry (CV) measurements of the LCPT29-based biosensor were performed at scan rates ranging from 25 to 200 mV s^{-1} over a potential range of −0.7 to +0.7 V vs Ag/AgCl. All experiments were conducted in a 5 mmol L^{-1} $[Fe(CN)_6]^{3-/4-}$ solution prepared in 10 mmol L^{-1} PBS buffer solution (pH 7.4), in the absence of PHB.

The modified electrode exhibited two well-defined redox peaks (Fig. 5), with peak currents increasing with the scan rate. The slight potential shift and the I_{pc} / I_{pa} ratio close to unity (1.03 at 100 mV s^{-1}, Table II) indicate quasi-reversible behavior.

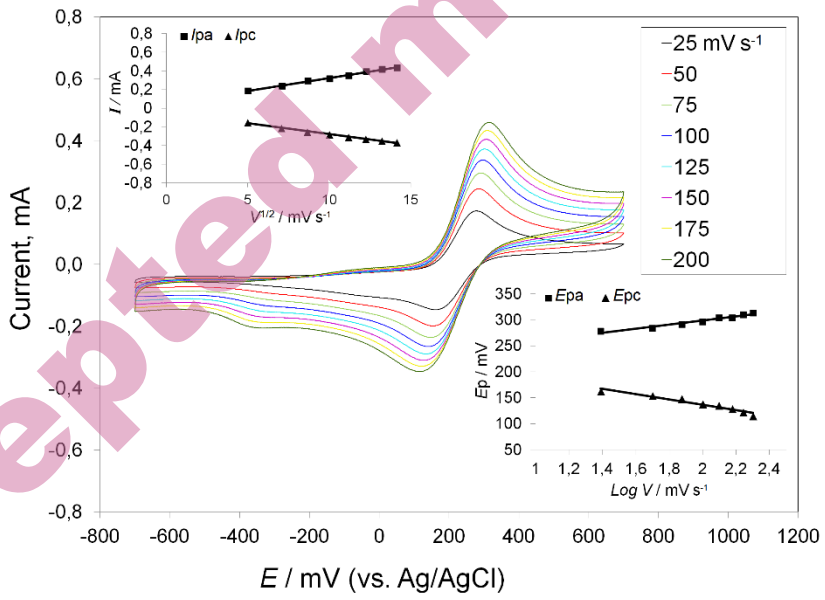

Fig. 5. Cyclic voltammograms of the modified electrode at scan rates from 25–200 mV s^{-1} over −0.7 to +0.7 V vs Ag/AgCl, using 5 mmol L^{-1} $[Fe(CN)_6]^{3-/4-}$ in PBS buffer (10 mol L^{-1} , pH 7.4). Insets show plots of anodic/cathodic current vs the square root of the scan rate and anodic/cathodic potential vs the logarithm of the scan rate.

TABLE II. Current and potential peaks analysis parameters recorded for the modified platinum electrode at different scan rates.

Scan rate, mV s^{-1}	I_{pa} / mA	I_{pc} / mA	$\lvert I_{pa} / I_{pc} \rvert$	E_{pa} /mV	E_{pc} / mV	ΔE_p / mV
25	0.162	-0.133	1.22	273	159	114
50	0.269	-0.214	1.26	284	154	131
75	0.333	-0.244	1.37	286	154	131
100	0.341	-0.311	1.03	294	143	151
125	0.428	-0.296	1.44	301	136	164
150	0.455	-0.311	1.46	304	122	182
175	0.493	-0.327	1.51	313	124	188
200	0.526	-0.348	1.51	313	115	199

The kinetic study of the effect of the scan rate on the anodic and cathodic peak currents (I_{pa} and I_{pc}) showed a linear relationship between the peak currents and the square root of the scan rate (Equations 1 and 2; inset Fig. 5), indicating a diffusion-controlled process.[38] The second inset of Fig. 5 reveals a linear dependence of E_{pa} and E_{pc} on the logarithm of the scan rate, as well as an increase in ΔE_p (Table II), confirming the quasi-reversible nature of the system.[13]

$$I_{pa} = 0.0276\, V^{½} + 0.0468 \qquad r = 0.9974 \qquad (1)$$

$$I_{pc} = -0.0231\, V^{½} - 0.0458 \qquad r = 0.9968 \qquad (2)$$

Concentration effect

The calibration curve developed to study the influence of analyte concentration on the response of the biosensor designed for the detection of PHB in aqueous media was established by successive additions of increasing concentrations (from 10^{-14} to 10^{-4} mol L^{-1}) to 100 mL of an electrolyte composed of 5 mol L^{-1} of $[Fe(CN)_6]^{3-/4-}$ in a 10 mol L^{-1} PBS solution. All measurements were carried out under optimized pH and temperature conditions, within a potential window ranging from −0.7 to +0.7 V. Prior to analyte injection, the electrochemical stability and repeatability of the biosensor were evaluated by recording fourteen consecutive cyclic voltammetry cycles in the presence of the immobilized enzyme and the redox mediator $[Fe(CN)_6]^{3-/4-}$. The negligible variation observed during these cycles confirmed the achievement of a stable and reproducible electrochemical response, thus ensuring reliable baseline conditions for subsequent calibration experiments. This behavior also suggests the absence of significant electrode surface passivation under the experimental conditions used.

As illustrated in Fig. 6a, the redox peak currents changed significantly with increasing PHB concentration, confirming the sensitivity of the modified electrode to PHB detection. The calibration curve (Fig. 6b) was constructed by plotting the absolute value of the cathodic peak current ($|I_{pc}|$) versus the logarithm of PHB concentration. The inset of Fig. 6b shows a strong linear relationship between the cathodic peak current and the logarithm of the PHB concentartion. According to

these results, this linear relationship is observed in the curve range from 10^{-14} to 10^{-8} mol L^{-1} (Equation 3). In contrast, a non-linearity between the current and the concentration was observed up to 10^{-8} mol L^{-1}, which could be due to saturation of the active site on the surface of the biosensor.[13]

$$I_p = 0.0327\ log\ C + 0.4908 \qquad r = 0.991 \quad (3)$$

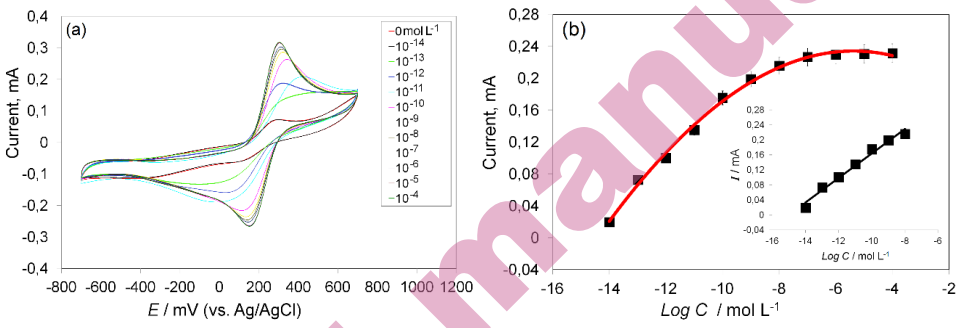

Fig. 6. Cyclic voltamograms of the LCPT29-based biosensor recorded at different PHB concentrations in PBS at optimal reaction conditions with the corresponding calibration curve of the cathodic peak current versus the logarithm of the PHB concentration (a and b, respectively). Error bars represent the standard deviation (n = 3).

According to this analytical curve, LCPT29-based biosensor demonstrated significant sensitivity (0.0327 mA L mol^{-1}) with a limit of detection (LOD) of 10^{-14} mol L^{-1}. In order to better evaluate the analytical performance of this biosensor, a comparative study was conducted with previously published studies (Table III).

Table III. Comparison of PHB detection characteristics with previously published studies using CV analysis.

Biosensor	LOD, mol L^{-1}	Linear range, mol L^{-1}	Optimum pH	Reference
1	1.0×10^{-14}	$10^{-14} – 10^{-8}$	8.0	This work
2	3.7×10^{-15}	$10^{-14} – 10^{-9}$	7.4	13
3	1.1×10^{-7}	$2.7 \times 10^{-8} – 1.07 \times 10^{-7}$	6.0	39
4	8.0×10^{-8}	$2.0 \times 10^{-6} – 20.0 \times 10^{-6}$	7.0	40

Effect of pH and temperature

pH and the temperature of the reaction medium are physico-chemical parameters that significantly influence enzyme activity. For example, in hydrolysis reactions, these two experimental parameters play a crucial role. pH generally affects the macromolecular stability of the enzyme protein, while temperature increases molecular collisions and improves the solubility of the substrate in the reaction medium.[41-44] It has been shown that, in the case of enzymes such as lipases, optimizing these two parameters is essential to ensure their stability and

maximize their enzymatic activity. Bacterial lipases are generally active in media with a wide pH range, from 3 to 12, and are thermostable between 30 and 60 °C.[45] These two parameters can also affect the response of a biosensor in terms of stability, and their optimization is therefore essential.[46]

For this purpose, we investigated the influence of these two physico-chemical parameters on the response of the developed biosensor in order to evaluate their effect. The experiments were conducted according to the previously mentioned operating protocol, at different temperatures between 20 and 50 °C, and by testing the reaction medium at different pH values (from 4 to 10). The response obtained at pH 7.4, corresponding to the initial experimental conditions, was included in Figure 7a as a comparative reference to evaluate the improvement achieved after pH optimization. To facilitate interpretation, the results of the CV analysis applied for this stage of the study are presented as graphs illustrating the evolution of the current peak versus pH and temperature (Fig. 7a–b, respectively).

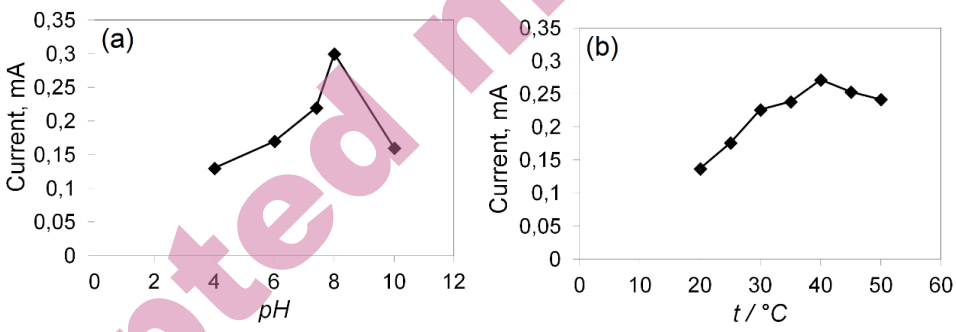

Fig. 7. Scatter plots of the current response (mA) of the biosensor as a function of pH and temperature (a and b, respectively). Experimental conditions: PBS (10 mM) ; PHB (10^{-7} M).

The results shown in Fig. 7a indicate that the current peak is highly dependent on the pH of the reaction medium. The biosensor response increases significantly between pH 4 and 8, while a marked decrease is observed at higher pH values. This reduction could be due to the accumulation of acidic products released during the reaction, which may locally lower the pH and create unfavorable conditions that reduce enzymatic activity and, consequently, the electrochemical response of the biosensor.[47]

The results presented in Fig. 7b indicate that the biosensor response increases with temperature between 20 and 40 °C, reaching a maximum at 40 °C due to increased enzymatic activity and reaction kinetics. Above this temperature, a significant decrease is observed, which could be attributed to enzyme denaturation or biomembrane degradation,[48] consistent with previous studies.[16,49]

Stability and selectivity of biosensor

The stability of the LCPT29-based biosensor was studied by subjecting the modified working electrode to fourteen successive cycles until the response stabilized. The results of the CV analysis were graphically represented by plotting the current (mA) versus cycle number (Fig. 8a) to better visualize the current response over successive cycles. Significant stability of the developed biosensor was observed, with a relative standard deviation (RSD) of 0.37% (< 5%). The selectivity of the developed biosensor was also evaluated by comparing different potential interfering substances (α-tocopherol and glycerol, phenol, bisphenol A, and cresol). α-Tocopherol and glycerol are frequently used in some industrial cosmetic formulations.[50,51] Phenol, bisphenol A and cresol were included among the relevant environmental pollutants frequently detected in industrial effluents and wastewater.[52,53] For consistency and reliable comparison, all interference experiments were conducted under the same experimental conditions previously optimized. The results were obtained by plotting the absolute value of the cathodic peak current versus the logarithm of PHB concentration (Fig. 8b). The significant reduction in the current signals recorded for the tested interfering substances confirms the high specificity of this biosensor for PHB.

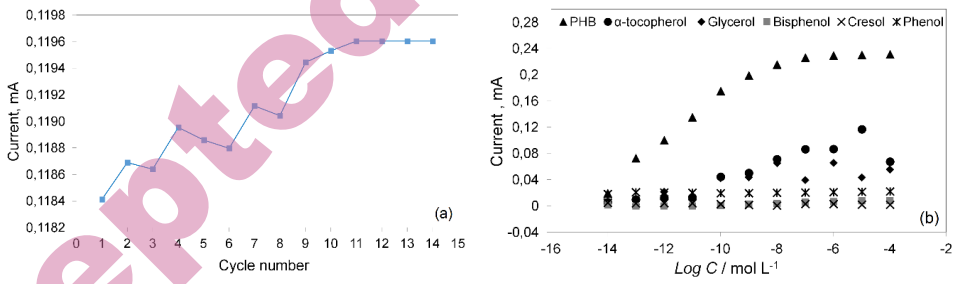

Fig. 8. Evaluation of stability and selectivity of LCPT29-based biosensor for sensing PHB in aqueous media (a and b, respectively).

Real sample validation of PHB

In order to evaluate the LCPT29-based biosensor performance in real matrices, recovery experiments were carried out using tap water and river water samples spiked with different known concentrations (from 10^{-8} to 10^{-11} mol L^{-1}) of the target analyte (PHB). The analyte concentrations in the real samples were determined using the calibration curve previously established with standard solutions by cyclic voltammetry (Equation 3), and the recovery values were calculated using Equation 4:[54]

$$Recovery = \frac{C_{\text{found}}}{C_{\text{added}}} \times 100 \quad (4)$$

				RSD, %
Tap water	0	–	–	–
	10^{-8}	$10^{-8.03}$	93.5	1.43
	10^{-9}	$10^{-9.02}$	94.8	1.06
	10^{-10}	$10^{-10.02}$	95.9	1.98
	10^{-11}	$10^{-11.01}$	97.3	2.52
River water	0	–	–	–
	10^{-8}	$10^{-8.04}$	90.8	1.50
	10^{-9}	$10^{-9.02}$	95.3	1.05
	10^{-10}	$10^{-10.04}$	91.4	2.10
	10^{-11}	$10^{-11.03}$	94.0	2.46

CONCLUSION

In this work, a native, detergent-stable lipase from the *Actinomadura Keratinilytica* CPT29 strain was deposited onto a platinum working electrode for the environmental detection of organic pollutants. The formation of the membrane network was confirmed by FT-IR spectroscopy and cyclic voltammetry (CV), demonstrating successful deposition on the platinum electrode. Under optimal experimental conditions, the enzyme membrane showed a markedly improved response for the detection of PHB as a model analyte, leading to a 30-fold increase in sensitivity compared to our previous study using a commercial lipase. The results obtained in this study are satisfactory, and the successful recovery in real water samples demonstrated the practical applicability of the biosensor, which has encouraged us to consider further work to more precisely evaluate its performance in different media and with different analytes, with the aim of enabling large-scale multisensory detection.

Acknowledgements: This work was generously supported by The General Directorate for Scientific Research and Technological Development (DG-RSDT), Algerian Ministry of Higher Education and Scientific Research.

И З В О Д

ВОЛТАМЕТРИЈСКО ИСПИТИВАЊЕ ПЛАТИНСКОГ БИОСЕНЗОРА СА ЛИПАЗОМ CPT29 ИЗ БАКТЕРИЈЕ *ACTINOMADURA KERATINILYTICA* УНАКРСНО ПОВЕЗАНОМ ПОМОЋУ GA/BSA И СТАБИЛНОМ НА ДЕТЕРГЕНТЕ

SELMA BOUNOUR[1], FATIHA BENAMIA[1], NOURA SEMACHE[1], SAIDA ZOUGAR[2], RAHMA BENYAHIA[2], NOUREDDINE DADDA[3], ALI LADJAMA[4]

[1]Laboratory of Applied Organic Chemistry, Chemistry Department, Faculty of Sciences, Badji Mokhtar University, P.O. Box 12, 23000 Annaba, Algeria, [2]Laboratory of Environmental Engineering, Process Engineering Department, Faculty of Technology, Badji Mokhtar University, P.O. Box 12, 23000, Annaba, Algeria, [3]Laboratory of Synthesis and Organic Biocatalysis, Chemistry Department, Faculty of Sciences, Badji Mokhtar University, P.O. Box 12, 23000 Annaba, Algeria, and [4]Laboratory of Applied Biochemistry and Microbiology, Biochemistry Department, Faculty of Sciences, Badji Mokhtar University, P.O. Box 12, 23000, Annaba, Algeria.

Ова студија описује имобилизацију нативне липазе (LCPT29) из соја *Actinomadura keratinilytica* CPT29, изолованог из живинског компоста у североисточном Алжиру, у сврху детекције естарских загађивача у воденој средини. У ту сврху, ова липаза стабилна у детергентима имобилизована је на платинску (Pt) електроду помоћу глутаралдехида као унакрсног везива, у присуству говеђег серумског албумина (БСА). Припремљена ензимска мембрана карактерисана је помоћу FT-IR спектроскопије, чиме је потврђено формирање њене мреже, као и њено наношење на платинску електроду кроз процену електрохемијских промена помоћу цикличне волтаметрије. Ефикасност радне електроде обложене унакрсно повезаном ензимском мембраном електрохемијски је процењена детекцијом пропил-4-хидроксибензоата (PHB) као модел-аналита. Под оптималним условима и при примењеном потенцијалу од –250 mV, биосензор на бази LCPT29 показао је линеаран одзив у опсегу концентрација од 10^{-14} до 10^{-8} mol L^{-1} (r = 0,991), са границом детекције од 10^{-14} mol L^{-1}. Биосензор је показао високу осетљивост (0,0327 mA L mol^{-1}), добру стабилност (RSD = 0,37%) и значајну селективност, као и могућност анализе трагова PHB-а у реалним узорцима воде, што доказује његов потенцијал за практичну примену.

(Примљено 7. марта; ревидирано 17. априла; прихваћено 23. јула 2026.)

REFERENCES

1. M. Tadesse, Y. Liu, *Catalysts* **15** (2025) 571 (https://doi.org/10.3390/catal15060571)
2. D. S. Dkhar, R. P. Swain, R. Dubey, G. K. Patel, P. Chandra, *Ind. Crop. Prod.* **233** (2025) 121336 (https://doi.org/10.1016/j.indcrop.2025.121336)
3. S. D. Wijayanti, L. Tsvik, D. Haltrich, *Foods* **12** (2023) 3355 (https://doi.org/10.3390/foods12183355)
4. K. Sonowal, P. P. Borthakur, K. Pathak, *Eng. Proc.* **106** (2025) 5 (https://doi.org/10.3390/engproc2025106005)
5. L. Qu, X. Zhang, Y. Chu, Y. Zhang, Z. Lin, F. Kong, X. Ni, Y. Zhao, Q. Lu, B. Zou, *Foods* **14** (2025) 1254 (https://doi.org/10.3390/foods14071254)

6. S. Feng, W. Guo, A. Ding, S. M. Parsa, J. Pan, D. Cheng, T. V. Tung, H. H. Ngo, *Chem. Eng. J.* **510** (2025) 161891 (https://doi.org/10.1016/j.cej.2025.161891)
7. X. Liu, C. Kokare. *Chapter 11 - Microbial Enzymes of Use in Industry. Biotechnology of Microbial Enzymes Production*, Goutam Brahmachari, Eds., Biocatalysis and Industrial Applications, Academic Press, 2017, pp. 267–298 (https://doi.org/10.1016/B978-0-12-803725-6.00011-X)
8. L. Aktar, M. L. Saha, *Bangladesh J. Bot*. **52** (2023) 979-988 (https://doi.org/10.3329/bjb.v52i4.70580)
9. H. Brockerhoff, R. G. Jensen, *Lipolytic Enzymes*, Academic Press, Inc., Mishawaka. New York, 1974, pp.330.
10. P. Desnuelle, *In The Enzymes*. 3rd ed., Boyer, Academic Press, New York, 1972, pp. 575–616.
11. N. A Al-Dhabi, A. K. M. Ghilan, G. A. Esmail, M. V. Arasu, V. Duraipandiyan, K. Ponmurugan, *J. Infect. Public. Health* **12** (2019) 549–556 (https://doi.org/10.1016/j.jiph.2019.01.065)
12. H. Treichel, D. Oliveira, M. A. Mazutti, M. Di Luccio, J. V. Oliveira, *Food Bioprocess Technol.* **3** (2010) 182–196 (https://doi.org/10.1007/s11947-009-0202-2)
13. L. Snani, S. Zougar, F. Benamia, I. Ghodbane, *Sen. Rev.* **41** (2021) 333–340 (https://doi.org/10.1108/SR-05-2020-0113)
14. G. Sun, X. Wei, D. Zhang, L. Huang, H. Liu, H. Fang, *Biosensors* **13** (2023) 886 (https://doi.org/10.3390/bios13090886)
15. Y. R. Maghraby, R. M. El-Shabasy, A. H. Ibrahim, H. M. E. S. Azzazy, *ACS Omega* **8** (2023) 5184–5196 (https://doi.org/10.1021/acsomega.2c07560)
16. N. Semache, F. Benamia, B. Kerouaz, I. Belhaj, S. Bounour, H. Belghith, A. Gargouri, A. Ladjama, Z. Djeghaba, *Acta Chim. Slov.* **68** (2021) 575–586 (https://doi.org/10.17344/acsi.2020.6401)
17. A. Habbeche, B. Saoudi, B. Jaouadi, S. Haberra, B. Kerouaz, M. Boudelaa, A. Badis, A. Ladjama, *J Biosci Bioeng* **117** (2014) 413–421 (https://doi.org/10.1016/j.jbiosc.2013.09.006)
18. S. Kurbanoglu, S.A. Ozkan, A. Merkoçi, *Biosens. Bioelectron.* **89** (2017) 886–898 (https://doi.org/10.1016/j.bios.2016.09.102)
19. G. Rocchitta, A. Spanu, S. Babudieri, G. Latte, G. Madeddu, G. Galleri, S. Nuvoli, P. Bagella, M. Demartis, V. Fiore, R. Manetti, P. A. Serra, *Sensors* **16** (2016) 780 (https://doi.org/10.3390/s16060780)
20. R. García-Morales, A. García-García, C. Orona-Navar, J. F. Osma, K. D. P. Nigam, N. Ornelas-Soto, *J. Environ. Chem. Eng.* **6** (2018) 710–717 (https://doi.org/10.1016/j.jece.2017.12.006)
21. J. C. Gonzalez-Rivera, J. F. Osma, *Biomed Res. Int.* **2015** (2015) 845261 (https://doi.org/10.1155/2015/845261)
22. J. I. Reyes-De-Corcuera, H. E. Olstad, R. García-Torres, *Ann. Rev. Food Sci. Technol.* **9** (2018) 293–322 (https://doi.org/10.1146/annurev-food-030216-025713)
23. M. M. Rodríguez-Delgado, G. S. Alemán-Nava, J. M. Rodríguez-Delgado, G. Dieck-Assad, G. Rocchitta, A. Spanu, S. Babudieri, G. Latte, G. Madeddu, G. Galleri, S. Nuvoli, P. Bagella, M. Demartis, V. Fiore, R. Manetti, P. A. Serra, *Sensors* **16** (2016) 780 (https://doi.org/10.3390/s16060780)
24. S. Erdemir, O. Sahin, A. Uyanik, M. Yilmaz, *J. Incl. Phenom. Macrocycl. Chem.* **64** (2009) 273–282 (https://doi.org/10.1007/s10847-009-9562-5)

25. N. Zehani, S.V. Dzyadevych, R. Kherrat, N. Jaffrezic-Renault, *Front. Chem*. **2** (2014) 44 (https://doi.org/10.3389/fchem.2014.00044)
26. Z. S. Abbas, G. M. Sulaiman, M. S. Jabir, S. A. A. Mohammed, R. A. Khan, H. A. Mohammed, A. Al-Subaiyel, *Molecules* **27** (2022) 4521 (https://doi.org/10.3390/molecules27144521)
27. S. Yang, Z. Lian, M. Wang, P. Liao, H. Wu, J. Cao, X. Tong, T. Tian, H. Wang, L. Jiang, *Ultrason. Sonochem*. **90** (2022) 106186 (https://doi.org/10.1016/j.ultsonch.2022.106186)
28. W. Zhong, L. Xu, Q. Wang, X. Shen, *J. Dairy Sci.* **108** (2025) 282–297 (https://doi.org/10.3168/jds.2024-25495)
29. D. Usoltsev, V. Sitnikova, A. Kajava, M. Uspenskaya, *Biomolecules* **9** (2019) 359 (https://doi.org/10.3390/biom9080359)
30. M. Chen, W. She, X. Zhao, C. Chen, B. Zhu, Y. Sun, Z. Yao, *Bioresour. Bioprocess*. **11** (2024) 7 (https://doi.org/10.1186/s40643-023-00721-9)
31. J. Liu, Y. Xu, S. Liu, S. Yu, Z. Yu, S. S. Low, *Biosens.* **12** (2022) 494 (https://doi.org/10.3390/bios12070494)
32. E. Keskin, M. Kiran, Y. Yardim, *J. Serb. Chem. Soc*. **00** (2026) 1-17 (https://doi.org/10.2298/JSC250718094K)
33. P. A. Serra, Ed.: *Biosensors for Health, Environment and Biosecurity.* IntechOpen Publishers, pp. 552 (https://doi.org/10.5772/928)
34. E. Djaalab, M. E. H Samar, S. Zougar, R. Kherrat, *Catalysts* **8** (2018) 233 (https://doi.org/10.3390/catal8060233)
35. O. Ouerghi, A. Touhami, N. Jaffrezic-Renault, C. Martelet, H. BenOuada, S. Cosnier, *IEEE Sens. J.* 4 (2004) 559–567 (https://doi.org/10.1109/JSEN.2004.832858)
36. N. Valkova, F. Lépine, L. Labrie, M. Dupont, R. Beaudet, *J. Biol. Chem.* **278** (2003) 12779–12785 (https://doi.org/10.1074/jbc.M213281200)
37. T. Koseki, K. Mihara, T. Murayama, Y. Shiono, *FEBS Letters* **584** (2010) 4032–4036 (https://doi.org/10.1016/j.febslet.2010.08.021)
38. S. Azzouzi, L. Rotariu, A. M. Benito, W. K. Maser, M. B. Ali, C. Bala, *Biosens. Bioelectron*. **69** (2015) 280–286 (https://doi.org/10.1016/j.bios.2015.03.012)
39. S.Y. Yahyaa, S. T. Ameen, K. K. Hashim, *J. Kufa Chem. Ssci.* **2** (2018) 93–114 (https://journal.uokufa.edu.iq/index.php/jkcs/article/view/3375)
40. L. F. De Lima, E. A. Pereira, M. Ferreira, *Sens Actuators B Chem.* **310** (2020) 127893 (https://doi.org/10.1016/j.snb.2020.127893)
41. S. Iqbal, M. Irfan, F. Tabassum, H. A. Shakir, J. I. Qazi, *J. Northeast Agric. Univ.* **24** (2017) 51–59
42. M. Morikawa, H. Daido, T. Takao, S. Murata, Y. Shimonishi, T. Imanaka. *J Bacteriol*. **175** (1993) 6459-6466 (https://doi.org/10.1128/jb.175.20.6459-6466.1993)
43. M. Sebatini, M. Jain, P. Radha, S. Kiruthika, K. Tamilarasan, *3 Biotech.* **6** (2016) 184 (https://doi.org/10.1007/s13205-016-0501-z)
44. S. Handayani, I. Novianingsih, A. Barkah, S. Hudiyono, *Makara. J. Sci.* **16** (2012) 141 (https://scholarhub.ui.ac.id/science/vol16/iss3/1)
45. K. Akhter, I. Karim, B. Aziz, A. Bibi, J. Khan, T. Akhtar, *PLoSONE* **17** (2022) e0273368 (https://doi.org/10.1371/journal.pone.0273368)
46. A. L. Campaña, S. L. Florez, M. J. Noguera, O. P. Fuentes, P. R. Puentes, J. C. Cruz, J. F. Osma, *Biosensors* **9** (2019) 41 (https://doi.org/10.3390/bios9010041)

47. Y. Chen, B. Fu, G. Xiao, L.Y. Ko, T.Y. Kao, C. Fan, J. Yuan, *ACS Food Sci. Technol*. **1** (2021) 382–387 (https://doi.org/10.1021/acsfoodscitech.1c00023)
48. R. Chokkareddy, N. K. Bhajanthri, G. G. Redhi, *Biosensors* **7** (2017) 21 (https://doi.org/10.3390/bios7020021)
49. Ş. Alpat, A. Telefoncu, *Sensors* **10** (2010) 748–764 (https://doi.org/10.3390/s100100748)
50. Z. Zou, L. Dai, D. Liu, W. Du *Catalysts* **11** (2021) 739 (https://doi.org/10.3390/catal11060739)
51. J. Kaura, A. Kumar Sarmab, M. K. Jhaa, P. Gera, *Biotechnol. Rep.* **27** (2020) e00487 (https://doi.org/10.1016/j.btre.2020.e00487)
52. J. Wang, L. Zhang, Y. He, R. Ji, *J. Hazard. Mater* **469** (2024) 133906 (https://doi.org/10.1016/j.jhazmat.2024.133906)
53. R. L. Ramos, V. R. Moreira, M. C. Santos Amaral, *J. Environ. Manage.* **351** (2024) 119772. (https://doi.org/10.1016/j.jenvman.2023.119772)
54. A. Ganash, S. Alshammari, E. Ganash, *Molecules* **28** (2023) 19 (https://doi.org/10.3390/molecules28010019)
55. A. Guo, P. Amini, C. Su, E. Sharma, J. Okoroma, J. O. Okeme, *Environ. Pollut*. **375** (2025) 126342 (https://doi.org/10.1016/j.envpol.2025.126342).